The Nature of Boxy/Peanut Spiral Galaxies: Overview and New Results

M. Bureau and K. C. Freeman

Mount Stromlo and Siding Spring Observatories, Institute of Advanced Studies, The Australian National University, Private Bag, Weston Creek P.O., ACT 2611, Australia
martin@mso.anu.edu.au, kcf@mso.anu.edu.au

Abstract: The formation mechanism of boxy/peanut-shaped bulges in spiral galaxies has been a problem for many years. We briefly review here the possible formation scenarios of boxy/peanut bulges, concentrating on both the bar-buckling and accretion hypotheses, and then describe an observational program aimed at testing those various theories and studying the vertical structure of edge-on bars. Our program includes optical long-slit spectroscopy, H I line-imaging, near-infrared imaging, and multi-band optical imaging. New spectroscopic results (both optical and H I) are presented on seven galaxies including five boxy/peanut-bulge spirals. Based on Kuijken & Merrifield's (1995) idea for detecting edge-on bars, we argue that these observations constitute a strong case in favour of the bar-buckling mechanism to form boxy/peanut-shaped bulges, but they also raise many questions and prompt for more detailed modelling to be made. The implications of the observations concerning the determination of rotation curves and of the physical conditions in bulges are also discussed.

Keywords: Galaxies: Formation — Galaxies: Evolution — Galaxies: Kinematics and Dynamics — Galaxies: Structure — Galaxies: Spiral — Instabilities

1 Introduction

Spirals constitute a large fraction of the giant galaxies and of the visible mass of the universe. Furthermore, a significant fraction of edge-on spiral galaxies, and therefore presumably of all spirals, show boxy or peanut-shaped isophotes in the bulge region. Because of the subjectivity involved in identifying boxy/peanut bulges, the fraction of bulges found to be boxy/peanut-shaped varies appreciably from study to study, but a typical number is 20-30% (Jarvis 1986: Shaw 1987; de Souza & dos Anjos 1987). Consequently, by their sheer number, boxy/peanut-bulge spiral galaxies constitute a significant class of object.

More importantly, boxy/peanut spirals display interesting characteristics. Firstly, the structure of boxy/peanut bulges represents a major departure from the usual $R^{\frac{1}{4}}$ density distribution of the more spheroidal bulges. Furthermore, it should be remembered that

for a bulge to produce boxy/peanut isophotes when seen edge-on in projection, its 3D volume density distribution must be even more distorted. Secondly, what makes boxy/peanut bulges really interesting from a dynamical point of view is that many of them are cylindrical rotators; that is, their rotation velocity is independent of the distance from the plane of the galaxy (see Kormendy & Illingworth 1982; Rowley 1986). In the more spheroidal systems, the rotation velocity decreases rapidly with height. Other features, although less common, are also displayed by boxy/peanut-bulge galaxies. Some of them show isophotal twist, usually taken as a signature of triaxiality, and some even show directly the presence of a bar when the boxy/peanut shape is seen at moderate inclination (e.g. for NGC 4442, see Bettoni & Galletta 1994). It is of course not possible to identify a bar with certainty from the morphology alone in a galaxy seen very close to edge-on. The range of structural and dynamical features displayed by boxy/peanut spiral galaxies supports the view that they are an important and interesting class of objects. Understanding their present structure and dynamics is therefore of fundamental importance, as these are the primary clues to their formation mechanism(s).

It should be noted that the bulge of the Galaxy also displays boxy isophotes, even in the extinction-corrected near-infrared images from the Diffuse Infrared Background Experiment (DIRBE) (Weiland et al. 1994). In addition, there is now evidence for the presence of a bar in the Galaxy: asymmetries in the bulge light distribution (e.g. Blitz & Spergel 1991; Weiland et al. 1994), non-circular gas motions near the Galactic center (e.g. Binney et al. 1991), asymmetries in star counts (e.g. Nakada et al. 1991) and kinematics in the bulge (e.g. Beaulieu 1996), high gravitational microlensing optical depth toward the Galactic bulge (e.g. Paczyński et al. 1994), etc. This represents an additional motivation to study the structure and dynamics of boxy/peanut-bulge spiral galaxies as we might learn greatly about our own Milky Way by studying them.

In § 2, we introduce the accretion and bar-buckling scenarios for the formation of boxy/peanut bulges. In § 3, our observational programs to study those galaxies and their goals are described. These include optical long-slit spectroscopy, H I line-imaging, near-infrared imaging, and optical imaging. New spectroscopic and H I observations of a few of our sample galaxies are presented in § 4, and their implications are discussed in § 5. We conclude briefly in § 6.

2 Boxy/Peanut Galaxies Formation Scenarios

Various scenarios have been proposed to explain the nature and formation of boxy/peanut-bulge spiral galaxies. Among other possibilities, May, van Albada, & Norman (1985) showed that the action of an external torque on a spheroidal system can produce a box-shaped bulge. We will concentrate here on two other mechanisms which have their own problems when faced with observations, but appear promising at the moment. We will describe those two mechanisms in the rest of this section.

2.1 Accretion Mechanism

The first scenario to form boxy/peanut bulges is through the accretion of material onto a host spiral galaxy. Binney & Petrou (1985) have shown that it is possible to generate

cylindrically rotating boxy/peanut bulges using a distribution function (specifying the phase-space density) approach. In addition to the dependence of the distribution function on the two integrals of motion E (energy) and L_z (angular momentum around the symmetry axis), orbits reaching a given height above the plane are favoured through a third integral, giving rise to the boxy/peanut shape when the bulge is seen in projection. Cylindrical rotation follows naturally. Rowley (1986, 1988) later showed that for a two-integral distribution function, a truncation depending on both E and L_z instead of a conventional high energy cut-off also leads to boxy/peanut cylindrically rotating systems.

Binney & Petrou (1985) argued that the best way to form the required distribution function is through slow accretion of material. If the orbit of a satellite galaxy with velocity dispersion much lower than its orbital speed decays toward a host galaxy with a decay time-scale much longer than the orbital time, the material shed by the satellite will naturally give rise to the required boxy/peanut bulge shape.

Clearly, a whole range of such scenarios is possible, from the accretion of one or more small satellites galaxies to the merger of two galaxies of similar size. However, accretion scenarios face several problems. Firstly, in order to form a boxy/peanut-shaped bulge, the accreted material must have a particular distribution of orbital energy and angular momentum. It seems unlikely that several small accreted satellite galaxies would all satisfy this criterion. The remaining satellites should still be visible, but they are not (Shaw 1987). Secondly, in the case of a large companion, the increased velocity dispersion and smaller decay time preclude the necessary clustering of the accreted material in phase-space, and the end result of the accretion won't be a boxy/peanut-shaped bulge (Binney & Petrou 1985). Thirdly, we believe the merger of two spiral galaxies (or one spiral and one small elliptical) can not account for the large number of boxy/peanut-bulge galaxies seen: such mergers would require fairly precise alignment of the spin and orbital angular momenta of the two galaxies, and this seems an unlikely route for the production of about 1/3 of spiral bulges.

It seems that the only viable accretion scenario left to form boxy/peanut bulges is through the accretion of a small number of moderate size companions. In fact, while boxy/peanut-bulge spirals are not found preferentially in clusters (Shaw 1987), the best examples of this class of object are seen in small groups (e.g. NGC 128). Therefore, while accretion is unlikely to be the primary formation mechanism of boxy/peanut galaxies, it is likely that it plays a role in *some* cases. This view is supported by the fact that the related X-shaped galaxies can be formed through the accretion of a satellite galaxy (Whitmore & Bell 1988; Mihos et al. 1995). Consequently, observers should look for evidence of accretion in boxy/peanut-bulge galaxies, and part of our observational program does that (see § 3). On the other hand, we should note that Shaw (1993) did not detect any arcs, shells, or filaments optically around boxy/peanut bulge spirals. This argues against any kind of recent accretion or merger models.

2.2 Bar Buckling Mechanism

The second and currently fashionable scenario proposed to form peanut/boxy bulges is through the buckling and thickening of a bar in a strongly barred spiral galaxy. The buckling or fire-hose instability was first considered by Toomre (1966) in an idealised

model: basically, if the vertical velocity dispersion in a disk is less than about a third of the velocity dispersion in the plane, buckling modes will develop. Toomre's (1966) results were confirmed by many authors (e.g. Fridman & Polyachenko 1984; Araki 1985).

Combes & Sanders (1981) were the first to associate the formation of boxy/peanut-shaped bulges in spiral galaxies with the thickening of a bar in 3D N-body simulations. Many groups have subsequently reproduced and developed those results (e.g. Combes et al. 1990; Raha et al. 1991). Basically, after the bar develops, it thickens, and when looking at the system edge-on, the bar appears boxy when seen end-on and peanut-shaped when seen side-on. Although the thickening of a bar can be caused by instabilities associated with resonances between the bar motion and the vertical oscillations of the stars (e.g. Combes & Sanders 1981; Combes et al. 1990), this effect is probably not dominant, and the primary cause of the thickening is more likely to be the buckling instability itself. Bar formation makes the orbits in the bar more eccentric and aligns their principal axes without greatly affecting the motion perpendicular to the plane. The bar then becomes unstable to buckling modes, buckles, and settles with an increased vertical velocity dispersion and thickness (e.g. Raha et al. 1991). Notwithstanding how the bar thickened, the final boxy/peanut shape is probably due to "orbit-trapping" around the 2:2:1 (banana and anti-banana) periodic orbit family (Pfenniger & Friedli 1991; Raha 1992; for the notation and an excellent review on the subject, see Sellwood & Wilkinson 1993).

The bar buckling scenario to form boxy/peanut-bulge spirals is attractive for many reasons. Firstly, the fraction of boxy/peanut-bulge systems among edge-on spirals is similar to the fraction of strongly barred spiral galaxies observed in more face-on systems, at least for early-type spirals ($\approx 30\%$, Shaw 1987). The statistics for later types are not as conclusive, probably because of difficulties in classifying their generally smaller bulges. Secondly, N-body simulations of buckling bars reproduce the cylindrical rotation seen in boxy/peanut bulges. Thirdly, with the buckling instability, even isolated galaxies can develop a boxy/peanut-shaped bulge. This is in agreement with the fact mentioned that boxy/peanut-bulge spirals are not found preferentially in clusters (Shaw 1987).

The mechanism discussed here also has its drawbacks. The main problem faced by the bar buckling mechanism is that the observed boxy/peanut bulges are usually shorter with respect to the scale of the host galaxy than are the strong bars seen in simulations, although no proper statistics have been compiled. Also, interactions between the bar, the disk (through spiral arm activity), and the bulge and dark halo components (through dynamical friction) might affect the evolution of the bar. Particularly, transfer of angular momentum from the bar to a spheroidal component can be very efficient (Sellwood 1980; Weinberg 1985). Recent results by Debattista & Sellwood (1997) have shown that massive halos with a high central density can slow down bars very effectively, although a number of effects that could decrease this efficiency have been suggested (Sellwood & Debattista 1997). It is interesting to note though that the bar keeps growing during the process, and the boxy/peanut appearance isn't affected. In addition, many ideas have emerged recently about how a bar can be destroyed (e.g. very violent buckling instability, interaction with a massive companion), but the presence or growth (due to bar-driven material) of a central mass concentration is the most promising mechanism. A relatively small mass at the center of the bar can rapidly destroy the bar by affecting the orbit families associated

with it (see e.g. Hasan & Norman 1990; Norman, Sellwood, & Hasan 1996).

Associated with those questions is the issue of the stability of spiral disks to bar formation. Most simulations start with an equilibrium disk unstable to bar formation. But, that instability is so quick to act that it is uncertain whether such a disk would have formed in the first place. Recent simulations by Mihos et al. (1995) suggest interactions and mergers as a possible way to excite strong bar modes in a dynamically *stable* disk. The bar can then buckle and give rise to a boxy/peanut-shaped bulge in the usual manner. This scenario couples the accretion and bar buckling mechanisms.

Despite the problems mentioned, the formation of boxy/peanut-shaped bulge spiral galaxies through the buckling of a strong bar in a disk is the mechanism favoured at the moment. It offers a natural and efficient way to form boxy/peanut bulges, and the qualitative predictions of the models agree with what is known at the moment about this class of object. In addition, this scenario offers numerous opportunities for observers to test its validity. A large part of the observational programs described in § 3 is related to this hypothesis, and the new spectroscopy results presented in § 4 are aimed directly at testing it.

3 Observational Program

The main goal of our observational programs is to determine which mechanism is at the origin of boxy/peanut-shaped bulges, particularly to test the accretion and bar-buckling instability scenarios which were discussed in the previous section (§ 2). In addition, if most boxy/peanut galaxies prove to be edge-on barred spirals, the data will be used to study the vertical structure of bars and seriously test 3D bar models observationally for the first time. We will briefly describe our sample of galaxies and then discuss each type of observations (optical long-slit spectroscopy, H I line-imaging, near-infrared imaging, and optical imaging) and the goals we are trying to achieve with each of them.

3.1 Finding the Objects: The Galaxy Sample

Our sample of galaxies is composed of 32 edge-on spirals, of which about 2/3 have boxy or peanut-shaped bulges and 1/3 have other various types of bulges for comparison purposes (spheroidal, ellipsoidal, and exponential). Most of the galaxies were selected from existing catalogues (Jarvis 1986; Shaw 1987; de Souza & dos Anjos 1987; Karachentsev, Karachentseva, & Parnovsky 1993) and they are all accessible from the south ($\delta \leq +15°$). In order to get enough spatial resolution in the long-slit spectroscopy but still have objects small enough to be practical to image with our near-infrared camera, we have selected objects with bulges larger than 0.′6 and total (disk) size smaller than about 7′ (at the 25 B mag arcsec^{-2} level).

3.2 Testing the Bar Hypothesis: Optical Long-Slit Spectroscopy

Although some features of an edge-on spiral galaxy can give an indication that the galaxy is barred (such as a plateau in the projected light distribution), the usual photometric criteria used to identify bars in spiral galaxies are useless when the galaxy is seen edge-

on. But, Kuijken & Merrifield (1995) (see also Merrifield 1996) have shown that it is possible to identify a bar in those edge-on systems based on the particular dynamics of barred spirals. They show that the gas in an edge-on barred spiral galaxy has a different position-velocity diagram (PVD) than the gas in an axisymmetric disk, and that the "figure-of-eight" seen in the PVD is a signature of triaxiality (see Fig. 1a). The origin of this feature is qualitatively easy to understand. The collisional nature of the gas implies that it follows closed non-overlapping and non-intersecting orbits (the gas would shock otherwise). In a barred potential, around corotation, there are no such orbits: the orbits are elongated and change orientation by 90° at corotation, therefore crossing each other. Thus, a gap will appear in the gas PVD of a barred spiral galaxy (compared to an axisymmetric spiral) due to the unavailability of orbits around corotation (see Fig. 1 in Kuijken & Merrifield 1995 and/or Fig. 3 in Merrifield 1996). Stellar absorption lines should show a weaker but similar behaviour. This feature can then be used to identify barred galaxies among edge-on spirals.

Consequently, the most important part of our observational program is optical medium-resolution long-slit spectroscopy. By taking long-slit emission-line spectra along the major axis of the sample galaxies, we can identify which of the sample galaxies are barred and indirectly test the validity of the bar-buckling formation scenario for boxy/peanut bulges. If no emission lines (e.g. H α, [N II]) are detected, we have to rely on stellar absorption lines. Because of the nature of our sample, we will be able to say if a boxy/peanut-shaped bulge necessarily implies the presence of a bar, and vice-versa.

The long-slit spectroscopic results will also shed light on other aspects of the sample galaxies' nature. For example, we will detect gas or stellar counter-rotation, we should be able to detect the presence of a nuclear bar, and we will be able to look for evidence of bar destruction (e.g. high velocity dispersion in the plane) in the galaxies where no bar is detected and hopefully learn about those destruction mechanisms. In addition, by covering a large wavelength range, we can obtain ratios of gas emission lines useful in diagnosing the physical conditions in the interstellar medium (ISM) of our galaxies. This is particularly interesting because we get information on small scales (e.g. nuclear activity) *and* large scales (e.g. shock excitation of gas in bars), especially since bars are often considered an efficient way to feed material to the central part of active galaxies.

Section 4.1 presents preliminary optical long-slit spectroscopy results for some galaxies in our sample. The observations are discussed in § 5.

3.3 Penetrating the Dust Barrier: H I Line-Imaging

Ideally, to study the vertical structure of bars/bulges, one wants to work with systems as edge-on as possible. This reduces the problems of deprojecting the light distribution of slightly inclined systems and removing the contamination of the bulge light by the superposed disk, an operation which is model dependent. It is therefore very important to have a few "perfectly" edge-on boxy/peanut-bulge galaxies in our sample. But, the absorption in the plane affects the observed profile of the emission lines in perfectly edge-on and dusty systems, and prevents the use of the Kuijken-Merrifield method to identify which systems are barred. The solution to this problem is to go to regions of the spectrum where the disk is optically thin, e.g. near-infrared or radio wavelengths.

In the near-infrared, the H Brγ emission line is well suited for this kind of work as the disk is probably optically thin at the K-band. Unfortunately, the line is quite weak in most galaxies and near-infrared spectrographs with adequate resolution are not common instruments. A more attractive solution to the absorption problem is to use line-imaging with a radio synthesis telescope. The H I (λ21 cm) line is ideal as even the very dusty edge-on spiral galaxies are probably optically thin at 21 cm. We can then get the velocity distribution through the dust lane all along the disk, and with a spectral resolution much higher than possible optically. Because of the 2D spatial coverage, we can also study the behaviour of the gas as a function of height above the plane. In addition, the H I data allow to directly look for evidence of accretion events (e.g. debris or tidal tails). Thus, information on the likelihood of both of the two formation mechanisms proposed for boxy/peanut bulges is obtained simultaneously. Section 4.2 presents preliminary results of H I line-imaging for one galaxy in our sample (IC 2531). Those observations are also discussed in § 5.

Although the optical spectroscopic data contain less information than the radio synthesis data, they remain our primary tool because radio synthesis observations are useful only for the largest and most H I-rich galaxies in our sample (limited spatial resolution and sensitivity).

3.4 Studying the Vertical Structure of Bars: Near-Infrared Imaging

Once the edge-on galaxies with a bar are identified by the Kuijken-Merrifield method, near-infrared K-band imaging allows the study of the vertical structure of the bars and the investigation of the problem of their thickness without being significantly affected by dust absorption. For the first time, the 3D models of barred spiral galaxies constructed over the years will be seriously tested. For example, we will be able to derive the shape and vertical scaleheight of the bar and disk separately, and study how those vary with radius and Hubble type. In a model where a peanut bulge grows out of the thickening of a bar, Sellwood (private communication) obtains scaleheights for the inner part of the bulge/bar, the end of the bulge/bar, and the outer disk in the approximate ratios 2:3:1. Very little is known observationally about those issues at the moment (Andredakis & Sanders 1994). It will also be possible to compare directly the lengths of the boxy/peanut bulges, in units of disk scalelength, with the predicted lengths of bars from simulations. As mentioned previously, this is one of the possible problems of the bar-buckling formation scenario. Because the light distribution obtained from near-infrared photometry is relatively unaffected by dust, it is also much better than the usual optical photometry when used to compare with the density distributions predicted by various models, as it is possible to extend the observations/models comparison into the inner disk region where absorption is usually a problem.

Although we are not presenting any near-infrared imaging results in this paper, the observations are well underway and look promising.

3.5 Testing the Accretion Hypothesis: Optical Imaging

Information on the stellar populations of the bulge, disk, and bar, and their approximate ages is very helpful in order to discriminate between the different scenarios proposed for the formation of boxy/peanut bulges. In particular, this allows to discriminate between the scenario where the boxy/peanut shape arises from the thickening of a bar (homogeneous stellar population and identical ages for the disk and bar/bulge) and the scenario where it arises from the accretion of satellites (different stellar populations and ages for the disk and bar/bulge). The necessary information can be obtained with multi-color photometry. Imaging in many bands is also needed to study the structure of the galaxies as the colors carry information on the M/L ratio of each component of the light distribution, and allow the contribution of each component of the galaxy to the mass distribution to be evaluated. We are at the moment doing B, V, I, and K-band photometry of the sample galaxies, and adding the U-band is being considered as it would help us break the age-metallicity degeneracy. An interesting application of this data is to study the vertical distribution of stellar populations, and try to understand how the disk stars map into bar/bulge stars when/if the bar buckling instability occurs. Obviously, the major problem faced when using the optical multi-color photometry is that it is strongly affected by dust absorption and can therefore be used reliably only in dust-free systems or far from the disk.

No optical imaging results are presented in this paper but again the observations are underway.

4 Preliminary Results

We will present here preliminary results illustrating the status of our project (as of September 1996). More galaxies have been observed, but not all data have been analysed yet.

4.1 Optical Emission Line Observations

We present new long-slit spectroscopic results for a few galaxies in our sample. The data were taken using the Double Beam Spectrograph on the 2.3 m telescope at Siding Spring Observatory. The spectra were centered on the Hα emission line in the galaxies (λ6563 Å at rest). The galaxies NGC 5746, NGC 6722, IC 4767, IC 5096, and NGC 4703 were observed with a 1752×532 SITE ST-D06A thinned CCD, while the observations of ESO 240-G 11 used a less sensitive 1024×1024 Loral CCD. All galaxies were observed with a $1\farcs8$ slit aligned with the major axis (just above the dust lane when present). The spectral resolution is about 1.1 Å FWHM (0.55 Å pixel^{-1}), and the spatial resolution is $0\farcs9$ pixel^{-1}.

The data were reduced in the standard manner within IRAF and rebinned to a logarithmic scale. In order to isolate the emission lines, the combined exposures were sky-subtracted and continuum-subtracted to produce the final spectra (some work remains to be done to get a better subtraction of strong sky lines, see e.g. Fig. 1a).

In the next few paragraphs, we will comment on our observational results for each of the galaxies analysed so far. A more general discussion concerning the implications of the observations will be given in § 5. In the figures, we show only the region of the spectrum

around H α, including the two [N II] lines (λ6548 Å and λ6584 Å at rest). Our goal here is to illustrate the range of dynamical features visible in our spectra, and to show what the signature of a bar in an edge-on spiral galaxy looks like (the "figure-of-eight" of Kuijken & Merrifield 1995). Each spectrum is accompanied by an image of the corresponding galaxy from the Digitized Sky Survey on the same scale to illustrate the range of galaxy types and morphologies we look at and to allow for a connection to be made between certain dynamical features and galaxy morphologies (e.g. "figure-of-eight" spectrum and boxy/peanut-shaped bulge).

- *NGC 5746 (Fig. 1a):*

  NGC 5746 is without doubt our most spectacular result so far. This is one of the two original galaxies used by Kuijken & Merrifield (1995) to test the signature of a bar on the PVD of an edge-on spiral galaxy. We confirm here their results, but with higher S/N data. NGC 5746 is an intermediate-type spiral and a prototype peanut-shaped bulge galaxy. It is nearby (1720 km s^{-1}) so the amount of spatial detail in the spectrum is quite exciting. For example, just outside the steeply rising inner part of the PVD, one can clearly see a dip in the upper part of the profile. The origin of this dip is not known. The line-splitting ("figure-of-eight") in the PVD is obvious, extending to about twice the peanut-length, and probably denotes the presence of a bar seen partially side-on. It is seen in all three lines (although superposed on the stellar absorption in the case of H α). In fact, it is also easily visible in the two [S II] lines at λ6717 Å and λ6731 Å (rest wavelengths). In addition, one can see the line ratios (e.g. ([N II] λ6584 Å)/(H α λ6563 Å)) varying with position along the major axis, suggesting that the physical conditions of the ISM are different in the bulge and disk regions.

- *NGC 6722 (Fig. 1b):*

  NGC 6722 is a peanut-bulge galaxy very similar to NGC 5746, but more distant (4626 km s^{-1}). Nevertheless, one can still see the "figure-of-eight" clearly, especially in the redder [N II] line. Again, the split in the lines extends to about two peanut-lengths, and the rise is very steep in the inner part of the bulge. We also see many H II regions in the disk.

- *IC 4767 (Fig. 1c):*

  IC 4767 also has a peanut-shaped bulge and is relatively distant (3600 km s^{-1}). Contrary to NGC 5746 and NGC 6722, it is an early-type spiral. No dust lane is seen and in fact no emission lines are readily visible in the spectrum before subtracting the bright continuum. After continuum-subtraction, however, the spectrum shows strong gaseous line emission in the very inner part of the bulge. No emission is detected in the outer part of the bulge or in the disk. While H α is strongly suppressed by the stellar absorption, [N II] (λ6584 Å) shows very rapidly increasing rotation in the center. The [N II] line does not show any features and it is not clear

where the line emission originates, although an inner disk like that seen in NGC 128 is the most probable explanation (Emsellem 1997).

- *IC 5096 (Fig. 1d):*

  IC 5096 is another intermediate-type spiral at moderate distance (3087 km s^{-1}). Although the bulge does not display a peanut shape, it does possess boxy isophotes. It also displays a clear, strongly split PVD in the [N II] line at 6584 Å. The extent of the line-splitting seems again to be about two bulge-lengths. This result is exciting and probably indicates the presence of a bar seen end-on. The line ratios in the inner bulge region also seem different than in the rest of the galaxy.

- *ESO 240-G 11 (Fig. 1e):*

  ESO 240-G 11 is a nearby (2843 km s^{-1}) late-type spiral with an extended disk and a very small flattened bulge. In fact, the bulge shape is hard to determine, as it blends with the disk. The PVD displays a typical late-type galaxy behaviour over most of its length: the peak (rotation curve) is slowly-rising in the inner parts and completely flat in the outer parts. But, again, the redder [N II] line shows structure in the bulge region and, despite the low S/N, a split in the line is seen (at least, the PVD does not behave as it should in an axisymmetric disk). Although no spatial variation in the line ratios is seen in the inner parts, the feature seen in the PVD remains a surprising and unexpected result.

- *NGC 4703 (Fig. 1f):*

  NGC 4703 is another relatively distant late-type spiral (4340 km s^{-1}). It has a flattened bulge embedded in an almost edge-on dusty disk. NGC 4703 is perfect to demonstrate the effect of dust absorption on our long-slit spectroscopy. The PVD shows a featureless slowly rising solid-body rotation curve. This is exactly what is expected from an optically thick rotating disk, as one can only see the light from an outer disk annulus (see e.g. Bosma et al. 1992). In galaxies with a strong dust lane like NGC 4703, the need to observe emission lines in a region of the spectrum where the disk is optically thin is obvious. Otherwise, the dynamics in the central regions of the galaxies is simply hidden from view.

4.2 H I Observations

We present here new results of H I radio synthesis observations of the galaxy IC 2531. The observations were carried out using the Australia Telescope Compact Array (ATCA) in the 6.0A configuration for a 12 hr period (1996 April 6). Observations in other configurations are planned to increase the S/N and get a better *uv* coverage. We used a 8 MHz bandwidth with 512 channels in each polarisation centered on the H I line in the rest frame of the galaxy. This yielded a velocity resolution of 3.3 km s^{-1} $channel^{-1}$, more than seven times better than the optical spectroscopy. The spatial resolution was about $6'' \times 12''$ ($\alpha \times \delta$).

The data presented here are extremely preliminary. They have not been edited, calibrated or cleaned: after subtracting the continuum, the data were directly imaged. Nevertheless, qualitative features are probably reliable.

Fig. 2 is similar to Fig. 1, showing a Digitized Sky Survey image of IC 2531 accompanied by its H I major axis position-velocity diagram. IC 2531 is a nearby (2477 km s^{-1}) late-type spiral with a small peanut-shaped bulge, an extended disk, and a strong dust lane. The H α spectroscopy shows strong absorption effects. The H I PVD in Fig. 2 extends to the limit of the optical disk. The rotation curve appears solid-body in the inner parts, but rises rapidly and flattens out in the outer parts, where there is significant structure: line-splitting is visible at least on one side of the galaxy. H I velocity profiles along the disk show the doubly-peaked nature of the profiles clearly. This feature is not visible in our optical spectrum and thus illustrate the usefulness of using radio synthesis imaging when dealing with galaxies with strong dust lanes. It should be noted that here, the split in the H I line starts at the end of the bulge and extends to almost five times its length. One should then ask if the origin of this feature is the same in IC 2531 as it is in galaxies like NGC 5746.

5 Discussion

The major goal of our observational program described in § 3 is to determine what is the formation mechanism of boxy/peanut-bulge spiral galaxies. Therefore, we will briefly discuss here the implications of the observations we have just described. While we only report on seven galaxies in this paper, our total sample comprises about 32 galaxies. Thus, our conclusions will be on much firmer ground when all our data is obtained, reduced, and analysed.

The NGC 5746 data we obtained (Fig. 1a) is so far unique. The PVD displays an enormous amount of detail; most interesting here, line-splitting is very strong in the inner regions and present in all the lines. Kuijken & Merrifield (1995) (see also Merrifield 1996) showed that this supports the bar buckling hypothesis by linking the line-splitting ("figure-of-eight") with the presence of a bar. Our NGC 5746 data confirm their observational results. The other boxy/peanut-shaped bulge galaxies NGC 6722 (Fig. 1b), IC 5096 (Fig. 1c), and IC 2531 (Fig. 2) also show double-peaked PVDs. The peanut-bulge galaxy IC 4767 (Fig. 1d) does not show line-splitting, but this might simply be due to the fact that the gaseous emission does not extend far enough in the disk. In fact, a hint of line-splitting is seen in the strong H α absorption line. In addition, for NGC 5746, NGC 6722, and IC 5096, the split in the emission lines (at least in [N II] at λ6584 Å) extends out to about twice the bulge (peanut) length. Considering that simulations suggest (e.g. Sellwood 1981, Combes & Sanders 1981) that corotation occurs just outside the end of the bar, associating the peanut shape with a bar is consistent with Kuijken & Merrifield's (1995) model which predicts that the line-splitting extends to about two corotation radius.

Before claiming detections of triaxiality, one needs to consider whether other structural or dynamical components in an axisymmetric spiral galaxy could give rise to a feature similar to the "figure-of-eight" in the gas PVD. The most obvious candidate is a ring embedded in an axisymmetric disk. The superposition of the apparent solid-body rotation

curve of an edge-on ring and an intrinsically more-or-less flat rotation curve would produce a double-peaked gas PVD, qualitatively similar to the gross features of the distribution shown in Fig. 1a for NGC 5746. We note, however, that the PVD for NGC 5746 is in detail much more complex than this simple picture would allow. Merrifield (1996: Figure 3) has shown that the PVD signature expected from an edge-on barred spiral galaxy can be similarly complex, depending on the viewing angle. It would be difficult to reproduce this level of complexity by simply adding or subtracting a dynamical component to an axisymmetric disk, a redistribution of the gas is really needed. In addition, a ring would produce a perfectly solid-body rotation curve, while the components of the PVDs observed are curved. Furthermore, rings can not account for PVDs of the type observed in IC 5096, where the "solid-body" component of the PVD is rotating faster than the disk. Therefore, based on Kuijken & Merrifield's (1995) and Merrifield (1996) work, we believe that our data represent the strongest case made so far in favour of the bar-buckling instability scenario to form boxy/peanut-shaped bulge spiral galaxies.

Although our data agree at least qualitatively with the modelling of Kuijken & Merrifield, some details are puzzling. First, the line-splitting region in the H I PVD of IC 2531 (Fig. 2) extends to about 5 peanut-lengths. Why is that? Many possibilities exist: maybe the H I does not trace the same structures as H α and [N II], maybe there is a very extended weak bar in the disk of IC 2531 giving rise to the extended line-splitting, maybe we are seeing the signature of strong spiral arms, ... IC 2531 is particularly interesting as it looks very much like the Galaxy. Therefore, pinpointing its structure and dynamics would help us greatly to understand our own Milky Way. Another interesting result is the structure seen in the PVD of the late-type galaxy ESO 240-G 11 (Fig. 1e). It does seem to show line-splitting in the inner regions, although the S/N is poor. This is unexpected as the bulge of ESO 240-G 11 is not boxy or peanut-shaped. Of course, ESO 240-G 11 could have a very weak bar in its disk, not giving rise to a boxy/peanut-shape structure, but still producing a split PVD. Such a possibility is hard to verify but would mean that thin bars do exist.

On a different note, our observations raise a worrying prospect concerning rotation curves of galaxies. In our long-slit observations, three galaxies out of the four that have structure in their PVD show a different behaviour in the H α and [N II] lines (the galaxies are NGC 6722, IC 5096, and ESO 240-G 11). For those three galaxies, in the region where a double-peaked PVD is seen in the [N II] λ6584 Å line, the H α line only shows the smaller rotation velocity peak (IC 5096 in Fig. 1c is the best example). This might simply be due to the fact that the H α line is superposed on the corresponding stellar absorption line. That idea is supported by the fact that we see an identical behaviour in the H α and [N II] lines only in the galaxy with the strongest emission lines (NGC 5746). Nevertheless, if we were to determine the rotation velocity of the gas from such data, without correcting for the stellar absorption, the [N II] line (unaffected by absorption) would yield a rapidly rising rotation curve which flattens abruptly at a relatively small radius, while the H α line (affected by absorption) would yield a slowly rising almost solid-body rotation curve which flattens out at a relatively large radius. The two rotation curves thus obtained would be significantly different, even on a qualitative level. This fact has at least two important consequences. First, many rotation curves derived in the conventional manner using the H α line might be wrong (at least for galaxies significantly inclined). Secondly,

if some rotation curves are wrong, the galaxies mass models based on them will be as well. Therefore, our understanding of galactic dynamics and structure based on those H α rotation curves could be seriously erroneous.

The observations also show the potential use of our data to determine the ionisation conditions and abundance of the gas in different regions of the galaxies, as we can measure the spatial behaviour of line ratios. Particularly, in addition to identifying nuclear activity, we can study large scale changes in the line ratios, such as those seen in some of our data where the whole bulge/bar region shows unusual physical conditions (NGC 5746 in Fig. 1a is the best example). Why does the [N II]/H α ratio change so much in those regions? This may prove a really interesting research direction to follow as we get data on more sample galaxies. Hopefully, we will learn something about the effects of bars on the ISM, and their relevance to the fuelling mechanism of active galaxies.

6 Conclusion

We believe that the observations reported in this paper, both long-slit spectroscopy and radio line-imaging, constitute the best observational indications up to now that the bar-buckling instability hypothesis to form boxy/peanut-shaped bulge spiral galaxies is correct. The previous evidence came mainly from imaging (*photometric* comparison with various models), but the strong line-splitting seen in the emission line spectra reported here agrees well with the *kinematical* predictions of Kuijken & Merrifield (1995) and Merrifield (1996) barred galaxy models. On the other hand, as much as our data support the bar-buckling scenario, they also raise many questions about the details of the models and their predictions. Our observations stress the need for more realistic models to be made, and for a better exploration of parameter-space, so that the models may be used to diagnose precisely the structure and dynamics of the galaxies. The question of how to discriminate between a bar and rings in an axisymmetric galaxy should also be addressed in more details.

Of course, the long-slit spectroscopy and H I line-imaging observations do not allow us to get a complete picture of the boxy/peanut bulge phenomenom, even when more sample galaxies are analysed. They mostly (but certainly not only) test the validity of the bar-boxy/peanut bulge association. Only when the optical and near-infrared imaging data are combined with the optical long-slit spectroscopy and the H I line-imaging data will we get, hopefully, a more complete picture of the structure, dynamics, and formation mechanism of this class of object.

Acknowledgements

We thank the staff of Mount Stromlo and Siding Spring Observatories and of the Australia Telescope National Facility for their assistance during and after the observations. We also thank A. Bosma and A. Kalnajs for useful discussions, and the referees for their helpful comments. M. Bureau acknowledges the support of an Australian DEET Overseas Postgraduate Research Scholarship and a Canadian NSERC Postgraduate Scholarship.

The Digitized Sky Surveys were produced at the Space Telescope Science Institute under U.S. Government grant NAG W-2166. The images of these surveys are based on photographic data obtained using the Oschin Schmidt Telescope on Palomar Mountain and the UK Schmidt Telescope. The plates were processed into the present compressed digital form with the permission of these institutions.

References

Andredakis, Y. C., & Sanders, R. H. 1994, MNRAS, 267, 283
Araki, S. 1985, Ph.D. Thesis, Massachusetts Institute of Technology
Beaulieu, S. 1996, Ph.D. Thesis, The Australian National University
Bettoni, D., & Galletta, G. 1994, A&A, 281, 1
Binney, J. J., Gerhard, O. E., Stark, A. A., Bally, J., & Uchida, K. I. 1991, MNRAS, 252, 210
Binney, J., & Petrou, M. 1985, MNRAS, 214 449
Blitz, L., & Spergel, D. N. 1991, ApJ, 379, 631
Bosma, A., Byun, Y., Freeman, K. C., & Athanassoula, E. 1992, ApJL, 400, L21
Combes, F., Debbasch, F., Friedli, D., & Pfenniger, D. 1990, A&A, 233, 82
Combes, F., & Sanders, R. H. 1981, A&A, 96, 164
Debattista, V. P., & Sellwood, J. A. 1997, em Dark Matter Conference 1996, in preparation
de Souza, R. E., & dos Anjos, S. 1987, A&AS, 70, 465
Emsellem, E. 1997, *The Nature of Elliptical Galaxies*, ed. M. Arnaboldi, G. Da Costa, & P. Saha, San Francisco: ASP, in preparation
Fridman, A. M., & Polyachenko, V. L. 1984, *Physics of Gravitating Systems*, (New York: Springer-Verlag)
Hasan, H., & Norman, C. 1990, ApJ, 361, 69
Jarvis, B. J. 1986, AJ, 91, 65
Karachentsev, I. D., Karachentseva, V. E., & Parnovsky S. L. 1993, Astron. Nachr. 314, 97
Kormendy, J., & Illingworth, G. 1982, ApJ, 256, 460
Kuijken, K., & Merrifield, M. R. 1995, ApJL, 443, L13
May, A., van Albada, T. S., & Norman, C. A. 1985, MNRAS, 214 131
Merrifield, M. R. 1996, *Barred Galaxies*, IAU coll. 157, ed. R. Buta, D. A. Crocker, & B. G. Elmegreen, San Francisco: ASP, 179
Mihos, J. C., Walker, I. R., Hernquist, L., de Oliveira, M. C., & Bolte, M. 1995, ApJL, 447, L87
Nakada, Y., Deguchi, S., Hashimoto, O., Izumiura, H., Onaka, T., Sekiguchi, K., & Yamamura, I. 1991, Nature, 353, 140
Norman, C. A., Sellwood, J. A., & Hasan, H. 1996, ApJ, 462, 114
Paczyński, B., Stanek, K. Z., Udalski, A., Szymański, M., Kałużny, J., Kubiak, M., Mateo, M., & Krzemiński, W. 1994, ApJL, 435, L113
Pfenniger, D., & Friedli, D. 1991, A&A, 252, 75
Raha, N. 1992, Ph.D. Thesis, University of Manchester

Raha, N., Sellwood, J. A., James, R. A., & Kahn, F. D. 1991, Nature, 352, 411
Rowley, G. 1986, Ph.D. Thesis, The Australian University
Rowley, G. 1988, ApJ, 331, 124
Sellwood, J. A. 1980, A&A, 89, 296
Sellwood, J. A. 1981, A&A, 99, 362
Sellwood, J. A., Debattista, V. P. 1997, Barred Galaxies and Circumnuclear Activity, Nobel Symposium 98, ed. Aa. Sandquist, P. O. Lindblad, & S. Jø"rster, (New York: Springer-Verlag), in preparation.
Sellwood, J. A., & Wilkinson, A. 1993, Rep. Prog. Phys., 56, 173
Shaw, M. A. 1987, MNRAS, 229, 691
Shaw, M. A. 1993, MNRAS, 261, 718
Toomre, A. 1966, *Geophysical Fluid Dynamics*, 1966 Summer Study Program at Woods Hole Oceanographic Institution, ref. no. 66-46, 111
Weiland, J. L., et al. 1994, ApJL, 425, L81
Weinberg, M. D. 1985, MNRAS, 213, 451
Whitmore, B. C., & Bell, M. 1988, ApJ, 324, 741

Figure 1–(a)-(f) Structure and kinematics of some sample galaxies. Top panel: Blue image of the galaxy (DSS). Bottom panel: Position-velocity diagrams (PVDs) of the ionised gas along the major axis of the galaxy. (a) NGC 5746, (b) NGC 6722, (c) IC 4767, (d) IC 5096, (e) ESO 240-G 11, (f) NGC 4703.

Figure 2–Structure and kinematics of IC 2531. Top pabel: Blue image of the galaxy (DSS). Bottom panel: H I position-velocity diagram along the major axis of the galaxy. The contours correspond to 1σ, 2σ, 3σ, 4σ, 5σ, and 6σ (not flux calibrated).

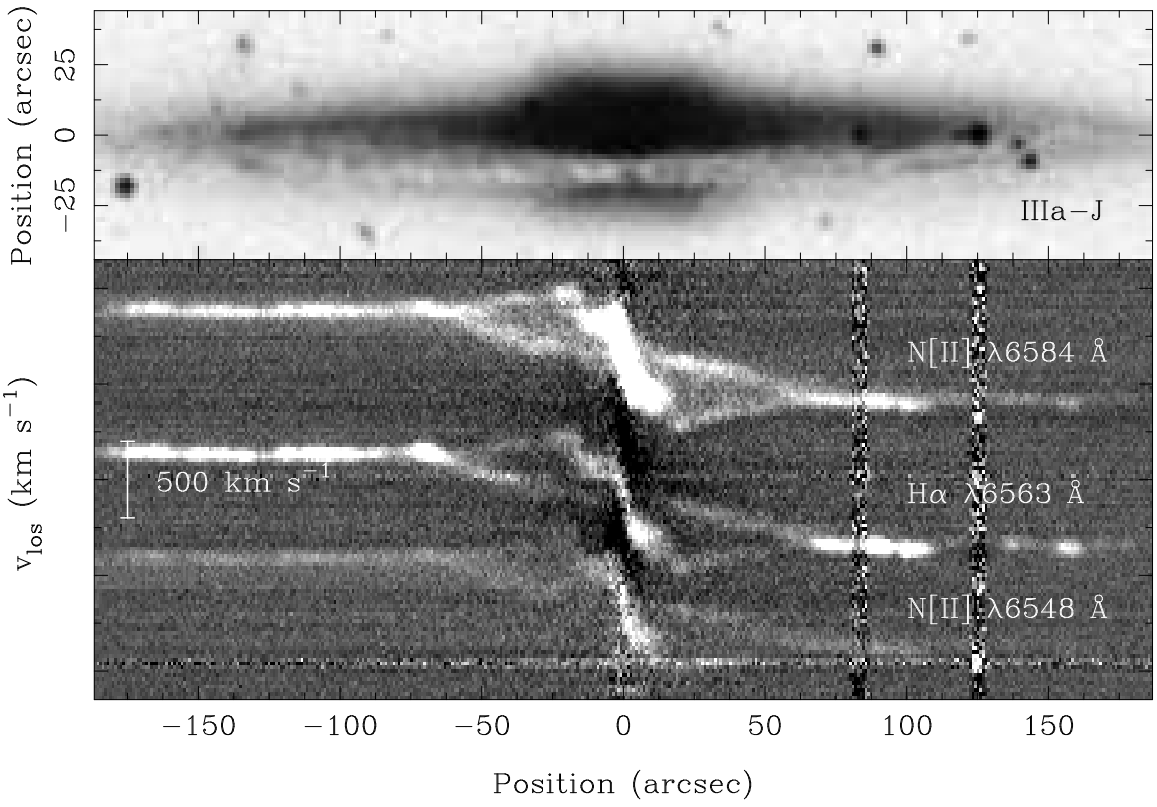
Position (arcsec)
25
0
−25
IIIa−J
N[II] λ6584 Å
Hα λ6563 Å
N[II] λ6548 Å
500 km s^{-1}
v_{los} (km s^{-1})
−150
−100
−50
0
50
100
150
Position (arcsec)

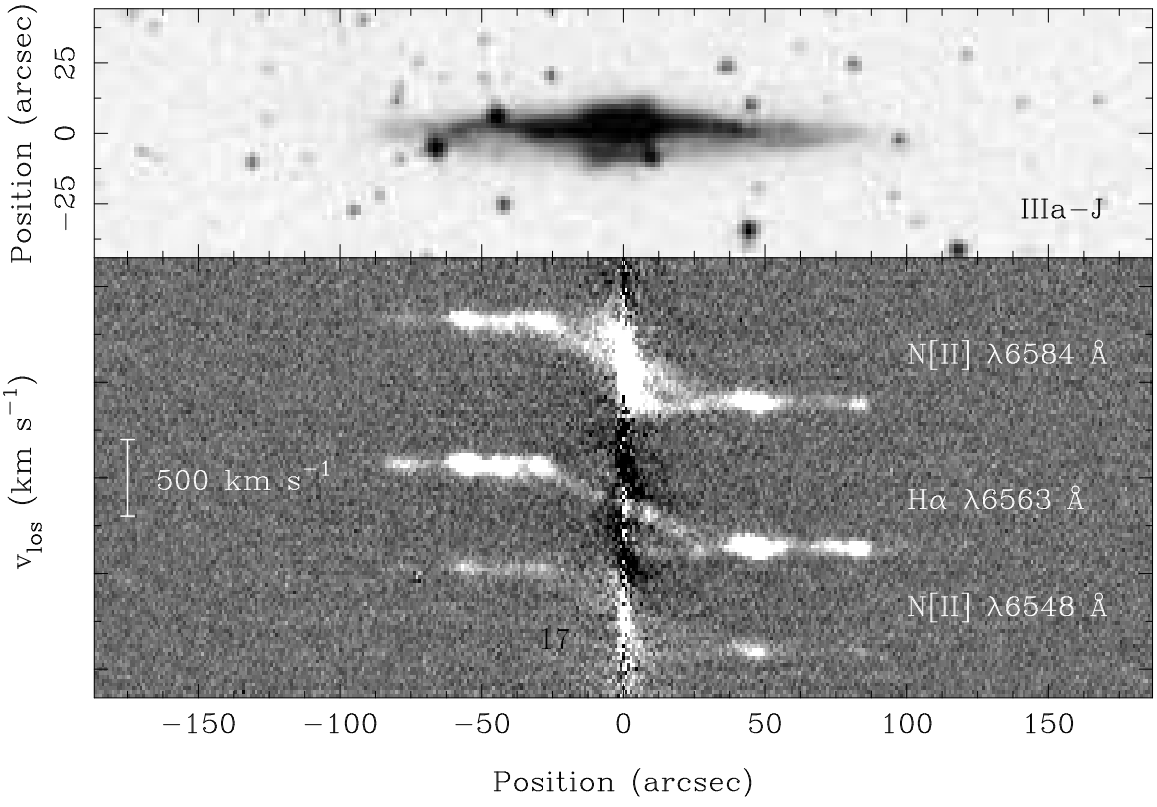
Position (arcsec)
25
0
−25
IIIa−J
N[II] λ6584 Å
Hα λ6563 Å
N[II] λ6548 Å
500 km s^{-1}
v_{los} (km s^{-1})
17
−150
−100
−50
0
50
100
150
Position (arcsec)

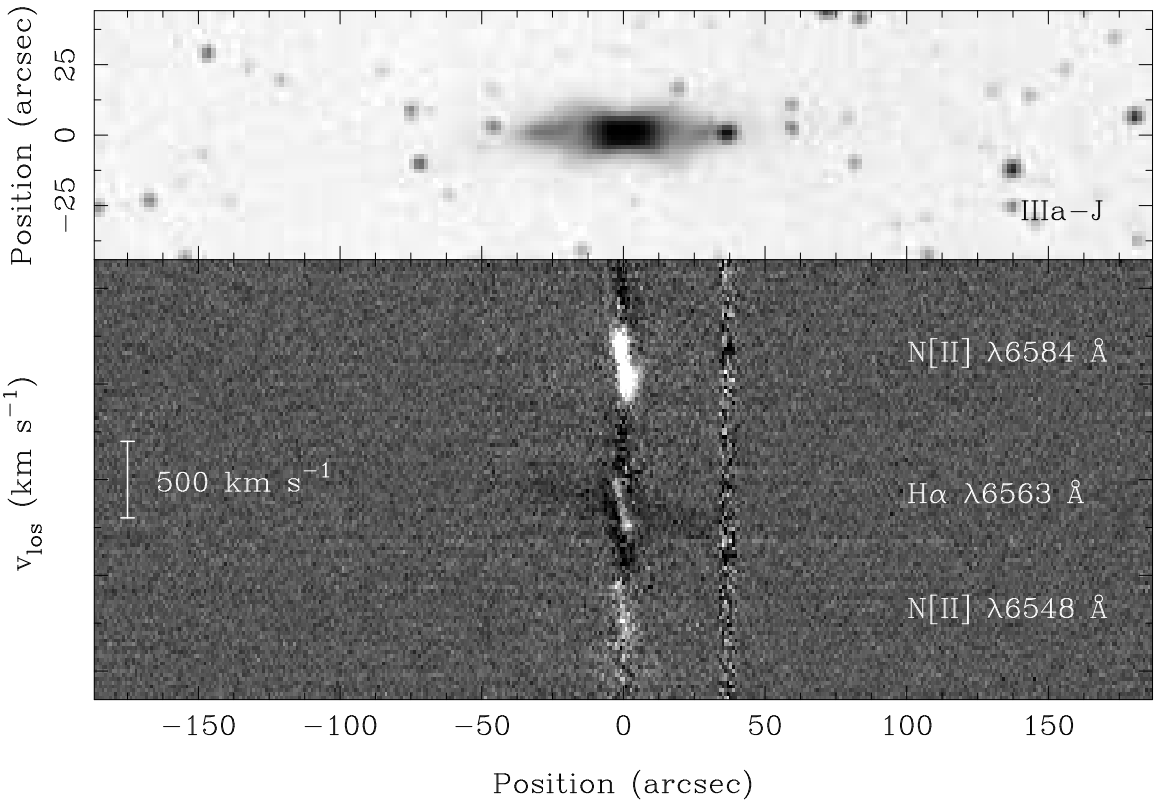
Position (arcsec)
25
0
−25
IIIa−J
N[II] λ6584 Å
Hα λ6563 Å
N[II] λ6548 Å
500 km s^{-1}
v_{los} (km s^{-1})
−150
−100
−50
0
50
100
150
Position (arcsec)

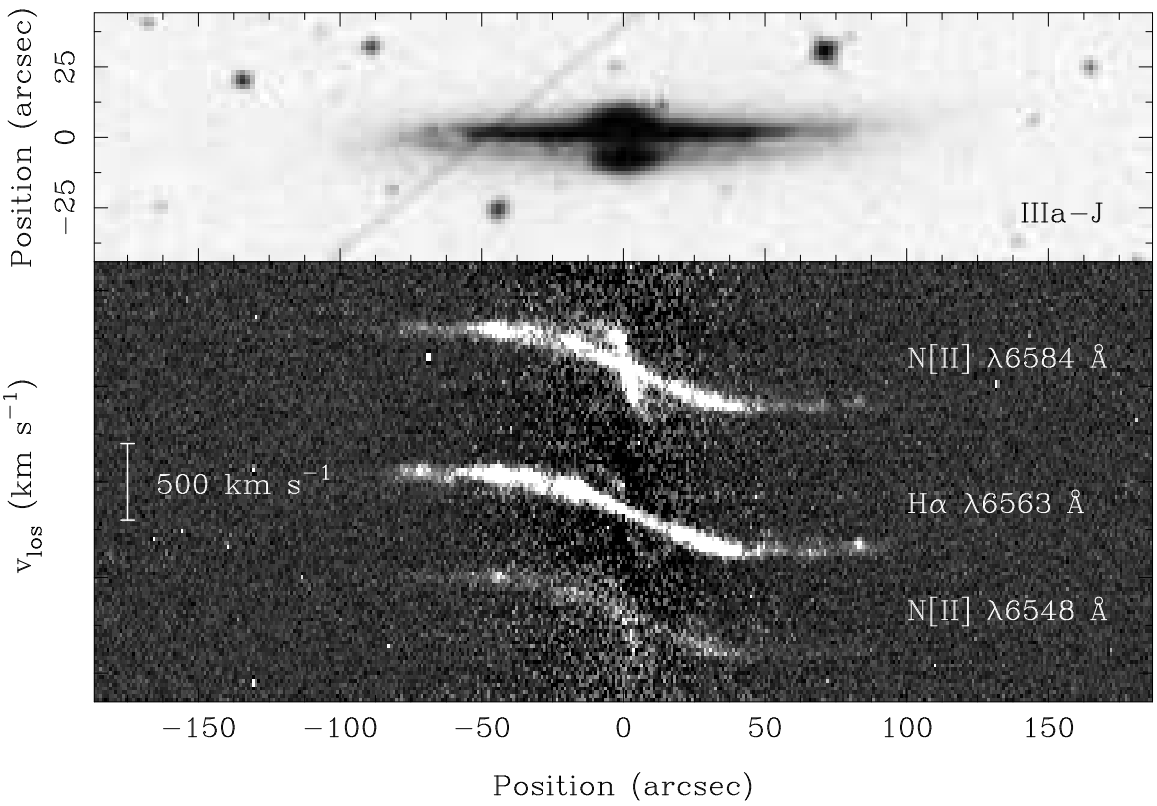
Position (arcsec)
25
0
−25
IIIa−J
N[II] λ6584 Å
Hα λ6563 Å
N[II] λ6548 Å
500 km s^{-1}
v_{los} (km s^{-1})
−150
−100
−50
0
50
100
150
Position (arcsec)

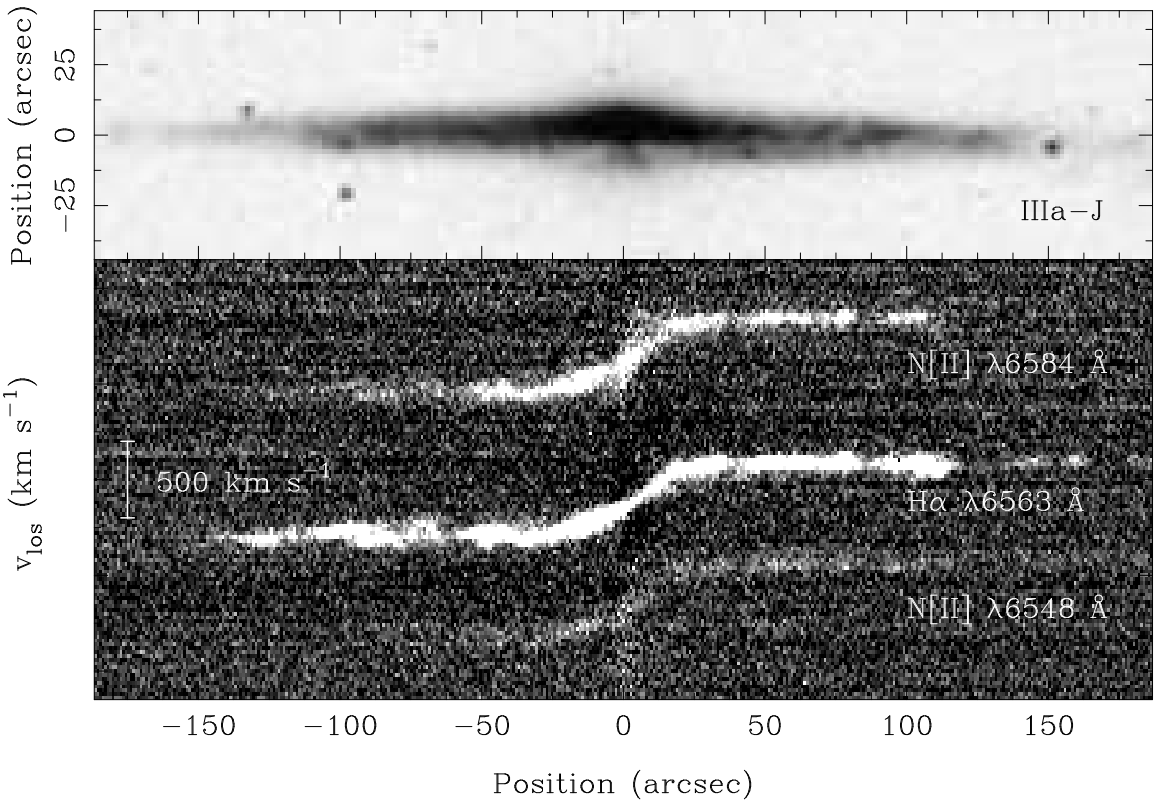
Position (arcsec)
25
0
−25
IIIa−J
N[II] λ6584 Å
Hα λ6563 Å
N[II] λ6548 Å
500 km s^{-1}
v_{los} (km s^{-1})
−150
−100
−50
0
50
100
150
Position (arcsec)

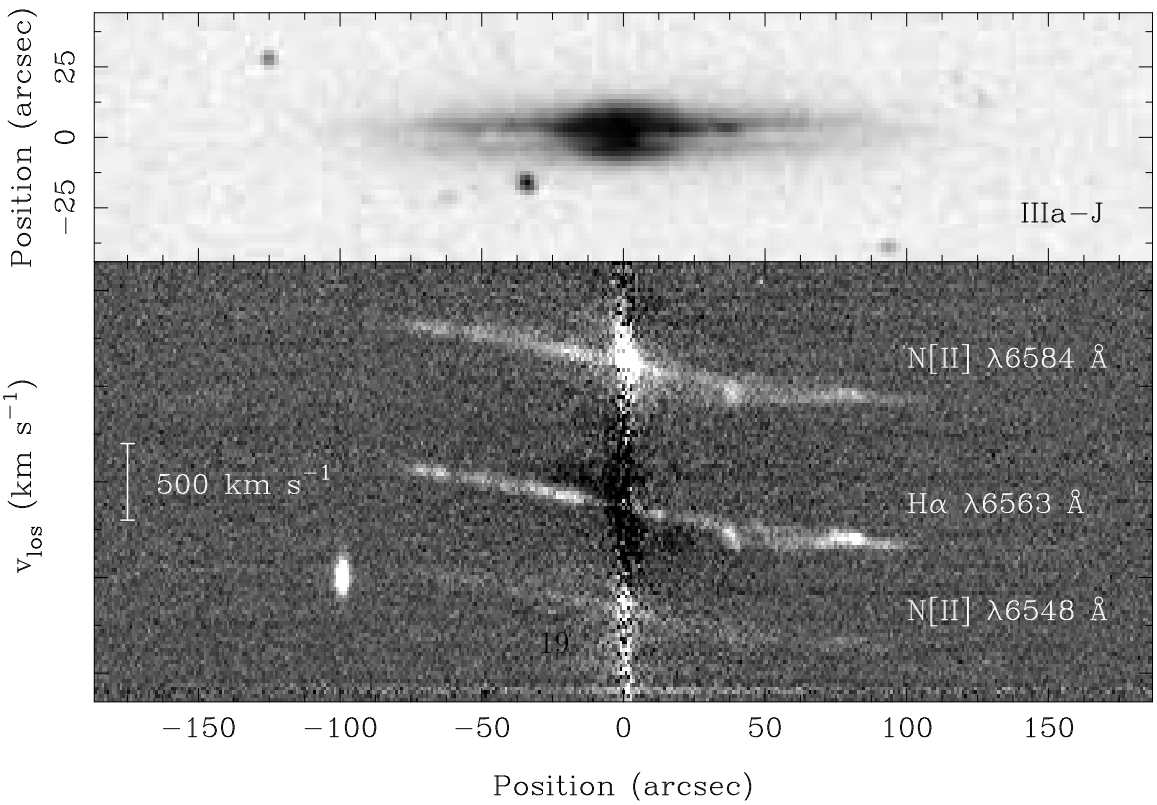
Position (arcsec)
25
0
−25
IIIa−J
N[II] λ6584 Å
Hα λ6563 Å
N[II] λ6548 Å
500 km s^{-1}
v_{los} (km s^{-1})
−150
−100
−50
0
50
100
150
Position (arcsec)

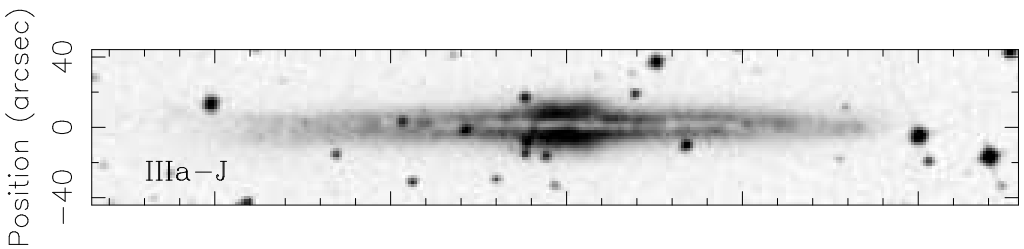
Position (arcsec)
40
0
−40
IIIa−J